



HAL
open science

A successful process to prevent corrosion of rich Gd-based room temperature magnetocaloric material during ageing

Madhu Chennabasappa, Michel Lahaye, Bernard Chevalier, Christine Labrugère, Olivier Toulemonde

► **To cite this version:**

Madhu Chennabasappa, Michel Lahaye, Bernard Chevalier, Christine Labrugère, Olivier Toulemonde. A successful process to prevent corrosion of rich Gd-based room temperature magnetocaloric material during ageing. *Journal of Alloys and Compounds*, 2021, 850, pp.156554. 10.1016/j.jallcom.2020.156554 . hal-02930065

HAL Id: hal-02930065

<https://hal.science/hal-02930065>

Submitted on 11 Sep 2020

HAL is a multi-disciplinary open access archive for the deposit and dissemination of scientific research documents, whether they are published or not. The documents may come from teaching and research institutions in France or abroad, or from public or private research centers.

L'archive ouverte pluridisciplinaire **HAL**, est destinée au dépôt et à la diffusion de documents scientifiques de niveau recherche, publiés ou non, émanant des établissements d'enseignement et de recherche français ou étrangers, des laboratoires publics ou privés.

A successful process to prevent corrosion of rich Gd-based room temperature magnetocaloric material during ageing.

Madhu Chennabasappa¹”, Michel Lahaye², Bernard Chevalier¹, Christine Labrugere² and Olivier Toulemonde^{1}*

¹ CNRS, Univ. Bordeaux, Bordeaux INP, ICMCB UMR 5026, Pessac, F-33600, France

² CNRS, Univ. Bordeaux, PLACAMAT UMS 3626, Pessac, F-33600, France

” Actual adresss Department of Physics, Siddaganga Institute of Technology, Tumakuru - 572103, India

When heat transport process occurs in a magnetic refrigeration device, magnetocaloric regenerator corrosion could be shed in light.. Our work mimicks this phenomenon by subjecting the magnetocaloric material $Gd_6Co_{1.67}Si_3$ to controlled water flow. The corrosion is first explained based on the elemental electrochemical oxidation thereby allowing a new test by the exposing material in passive fluid (KOH) up to 1 year. The neglected degradation of the material was justified by X-Ray photoelectron spectroscopy (XPS) and depth profile Auger spectroscopy, and thus the control of its corrosion is reported. The effective control of the corrosion when material is exposed to KOH could be a universal procedure in magnetic refrigeration prototype.

Keywords: *magnetocaloric, intermetallics, corrosion, photoelectron spectroscopies*

Corresponding Author **olivier.toulemonde@icmcb.cnrs.fr*

Introduction

Durability due to the combination of performance and consistency is the preliminary figure of merit for any device with promising potential application. In this regard, it is always requested to test the material for long and/or repeated working cycle before launching it into a working device. Our approach is dedicated for one such test on materials highlighted for use in *room temperature magnetic refrigeration (RTMR)*. RTMR has gained interest in the last decade or so as magnetic refrigeration is promising in terms of energy consumption, safety and efficiency. More importantly it is believed to be good replacements/alternatives for present days gas compressor based domestic refrigeration [1]. The magnetic refrigeration is based on the so called magnetocaloric effect (MCE) referring to a temperature change of a material when it is exposed to a change of the applied magnetic field [2]. One of the most commonly practiced measurements to evaluate it is to calculate the magnetic entropy change during the magnetic transition. Through Maxwell's relations around a second-order paramagnetic to ferromagnetic phase transition [3], magnetic entropy change given by the following equation (i) is related with the adiabatic temperature change of the material denoted in (ii)

$$\Delta S_M(T, H_1 \rightarrow H_2) = \int_{H_1}^{H_2} \left(\frac{\partial M}{\partial T} \right)_{p,H} dH \dots (i), \quad \Delta T_{ad}(T, H_1 \rightarrow H_2) = \int_{H_1}^{H_2} \frac{T}{C_p} \left(\frac{\partial M}{\partial T} \right)_{p,H} dH \dots (ii)$$

Where, dH corresponds to a change in two different applied magnetic fields H_1 & H_2 , ∂M is change in magnetization corresponding to temperature change of ∂T and C_p is the heat capacity of the material at a given temperature. Based on high values of magnetic entropy change and/or the adiabatic temperature change, there have been a lot of new materials put forward as potential for room temperature applications from different classes of materials such as oxides and intermetallics [4]. The number of publications involving the term “magnetocaloric effect” increased from about 50 publications per year in 2004 to more than 500 publications per year since 2014, a tenfold increase in a span of ten years [5]. At same time, there was steep increase in the number of magnetic refrigeration prototypes proposed by different scientists and engineers around the globe [6, 7]. Such developments showcase the increase in interest by a large magnitude of researchers in the field. The so developed prototypes take care of the feasibility of the material, the strength of the applied magnetic field, the nature of the heat transport fluids and other critical criteria from the point of application of magnetic refrigeration in domestic applications [8].

From a magnetocaloric refrigeration system point of view, the regenerator could be constructed in such a way that the heat transfer fluid might be in contact or not with the

magnetocaloric material. When direct contact occurs, it needs to be as large as possible to improve the heat transfer from regenerator to the fluid. But in that case, the MCE material in the regenerators is also subject to erosion and/or chemical corrosion. There is, therefore, one major concern that needs to be addressed with magnetocaloric materials: *the effects of heat transfer fluid on the chemical and physical stability of the regenerator*. Even though such effects are expected, surprisingly not much are systematically addressed. There are very few efforts to explore the durability of these materials once put into functional units [9, 10] and most of them are focused on $\text{LaFe}_{13-x}\text{Si}_x$ -based materials as highlighted in a recent publication [11]. For ensuring the chemical stability and avoiding deterioration of the refrigerant performance, some study suggested a surface protection process of the magnetocaloric materials by coating [9,12]. As a first step, one better believes that a detailed study of the working fluid effect on the magnetocaloric material with duration of exposure often addressed as *ageing* should help in understanding corrosion prior to suggesting any coating and/or passivation layer formation. It may also allow suggesting some alternative on the magnetocaloric refrigeration device design. Our choice is focused on one of the Gd rich materials i.e. $\text{Gd}_6\text{Co}_{1.67}\text{Si}_3$. It is because Gd rich materials and Gd metal itself are used as prototype material in the most of the room-temperature magnetic refrigerators [6] and because we initiated the magnetic properties study of this solid [13].

For the heat transport fluid, water is one suggestion and there are several commercialized, or not, options available which have their own uniqueness and advantages. Nevertheless, water is considered as an almost perfect fluid regarding its excellent heat transfer, its health and safety character and its low cost. However, one of the major problems is its freezing point ($^{\circ}\text{C}$), so that few suggest the use of one anti-freezing agent such as salt (CaCl_2 , MgCl_2 , LiBr , etc.), alcohols, glycols or non-aqueous fluids (mineral oils, synthetics) to overcome this. One of the comparatively safe, stable and low cost solutions is the mixture of ethanol and de ionized (DI) H_2O . Such mixing is also believed to reduce the surface tension. Having all this in mind, DI H_2O was first chosen to study its direct surface effect on our $\text{Gd}_6\text{Co}_{1.67}\text{Si}_3$ material showing moderate room temperature magnetocaloric properties [13]. A core-shell phenomenon at the surface of this ternary silicide when water flux ageing acts for 3 months was recently underlined resulting in a chemical selective corrosion process [14]. Remarkably unaltered bulk magnetocaloric effect was shown suggesting a passivation action of the top layer containing the paramagnetic Gd_2O_3 oxide [14].

Our work here was aimed at checking the suggested passivation activity of the micron length of the Gd_2O_3 layer on $\text{Gd}_6\text{Co}_{1.67}\text{Si}_3$ during extended time. Ageing process under DI H_2O exposure was extended up to 1 year thanks to a homemade device shown in Figure S 1. The material was shaped in regular form of thin slabs and was subjected to the effect of the DI H_2O flux. The sample has regularly been characterized for changes in the microstructure using microprobe, depth profile and X-Ray photoelectron spectroscopy, the nuclear structure using X-Ray diffraction and magnetization measurements. Finally, the same procedure was followed for the same material but this time under KOH flow exposure.

2. Experimental section

High purity elements of Gd (99%), Si (99.9%) and Co (99.9%) in a stoichiometric ratio were arc melted in pure argon atmosphere to obtain ingot of $\text{Gd}_6\text{Co}_{1.67}\text{Si}_3$. Ingot was arc melted twice by reversing each time to obtain homogeneity. Later this ingot was subjected to annealing at 800 °C for period of a month. For performing ageing slices of approximately 8 x 4 x 2 (l x b x h) mm were subjected to constant flux of DI water that was pumped into the sample chamber from a water reservoir using aquarium pump as shown in Figure S1 (a), details were already reported in our previous manuscript [14].

X-ray diffraction on Philips 1050 diffractometer were employed to confirm phase purity of samples on the as prepared slice and/or to follow the ageing effect on the aged slices. MPMS Squid was used for the magnetic measurements. VG microlab 310 F Auger electron spectroscopy was used for depth profile analysis. Elemental analysis was performed on CAMECA SX 100 (Bruker AXS) EPMA (Electron Probe Micro Analyzer) instrument equipped with three spectrometers namely, Wavelength-Dispersive Spectroscopy, Energy-Dispersive Spectroscopy and Silicon Drift Detector. X-ray photoelectron spectroscopy (XPS) data were collected on VG Scientific ESCALAB spectrometer using $\text{AlK}\alpha$ monochromatic source working at 70 W inside Ultra High Vacuum (UHV) chamber with working pressure of 10^{-7} Pa. Initially full spectra (0-1350 eV) were collected with constant energy of 150 eV and high-resolution spectra for specific element were obtained with constant energy of 40 eV. For analyzing the deeper layers of the sample, slides were in purpose scrapped with razor blade inside the UHV chamber.

3. Results and discussion

3.1 Water flux ageing action for 1 year

Figure 1 displays the photo snaps of starting/pristine and 1 year DI water aged samples: it roughly underlines the action of the water flux for 1 year on the $Gd_6Co_{1.67}Si_3$ material. Unambiguous change of the color and a loss of brightness are a result of chemical bonding nature changes at the material surface. The roughness of the 1 year DI water aged sample is related to the chemical corrosion and physical erosion. Related to our previous report [14] an increase of the XRD patterns intensity of the Gd_2O_3 top layer material can also be underlined (not shown here) resulting from an extended corrosion when the water flux action is increased in time. The corrosion is likely to be continuous in time and then no passivation phenomenon would occur in the given experimental condition.



Figure 1: Shape in centimetric range, color and roughness change of $Gd_6Co_{1.67}Si_3$ material when water flux acts for 1 year

Based on these results, magnetic and magnetocaloric properties were carried out. Collected and treated data are shown in figure 2a & 2b respectively. The effect of the time extension for the water flux action is studied and data for one-year ageing are compared with these collected for the 3 month aged sample. It is recalled that the ones' for the 3 month ageing sample perfectly matched with these of the virgin/starting material even if a micron length oxide layer was found on the top surface material after 3 months of ageing in water [14]. The magnetization data collected under 100 Oe were divided by the mass of probed materials including $Gd_6Co_{1.67}Si_3$ material embedded in oxidized layers of unknown depth for the 1 year aged sample. Figure 2a underlines a clear decrease of the magnetization plateau under 100 Oe keeping the intrinsic paramagnetic to ferromagnetic phase transition at 300K. It implies a reduction in the content of $Gd_6Co_{1.67}Si_3$ material with respect to the content of on top oxide layer that consequently does not act as a passivation layer. Oxide thickness increases with time of exposure. Figure 2 b shows the temperature dependence of the magnetic entropy change around the ferromagnetic transition. A decrease of about 15% of the overall entropy change is highlighted.

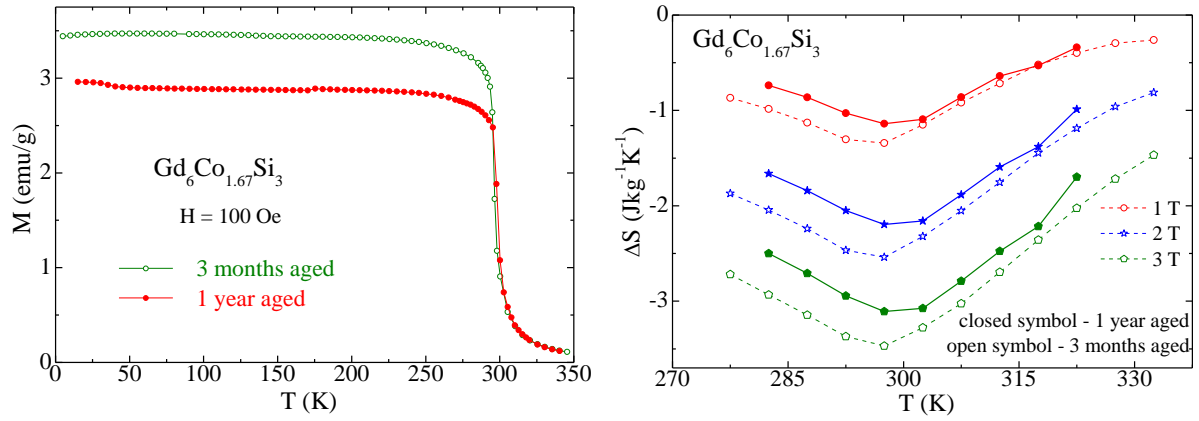


Figure 2: Temperature dependence magnetization curves of 3 months and 1 year water aged samples (a, left), Magnetic entropy change collected under 3 different applied magnetic fields from 1 to 3 Tesla for the two same samples (b, right).

3.2 Water with KOH as flux and the ageing action for several months up to one year

Only a pictorial representation and electrochemical reactions expected by spontaneous electrochemical reaction are summarized in Table S 1 for clarity because these items are detailed in our previous study [14]. The triggering of the complete corrosion is the dissolution of $\text{Co}^{2+}_{\text{aq}}$ resulting from the spontaneous oxidation reaction of the metallic cobalt content on $\text{Gd}_6\text{Co}_{1.67}\text{Si}_3$ material as following $2 \text{Co}_{\text{solid}} + \text{O}_2_{\text{gas}} + 2 \text{H}_2\text{O} \rightarrow 4 \text{OH}^-_{\text{aq}} + 2 \text{Co}^{2+}_{\text{aq}}$ (Equations 1 and 2 in Table S 1). Similar reactions occur between water and metallic Si (equations (1) and from (3) to (5)) and/or water and metallic Gd (equations (1) and (6)). That is why aqueous Co^{2+} and SiO_3^{2-} were previously found in the DI water used for testing [14]. Here, our approach aims to arrest the reaction involving Co^{2+} aqueous form. Accordingly, referring to the cobalt Pourbaix diagram, one can stop the corrosion by achieving the cobalt *immunity region* applying a low voltage to the material. However, this approach is not possible with respect to our test procedure. And, it is further not the best suggestion taking also into account the additional energy consumption increase that is required. Another option is to increase the pH value to those allowing achieving the *passivation region*. This second option should facilitate $\text{Co}(\text{OH})_2$ precipitation on surface following the redox equation $2\text{Co}_{\text{solid}} + \text{O}_2_{\text{gas}} + 2\text{H}_2\text{O} \rightarrow 2\text{Co}(\text{OH})_2_{\text{solid}}$. Such cobalt hydroxide would be formed on the top surface of the material and could act as protective layer for Si and Gd elements.



Figure 3: Shape, color and roughness change of 3 months aged $Gd_6Co_{1.67}Si_3$ material in KOH $pH \geq 12$ (left), in DI H_2O $pH \approx 7$ (right) .

The gadolinium based intermetallic was then aged under a flux of KOH solution with $pH \geq 12$ to verify and/or confirm the above proposed hypothesis. After ageing the sample for 3 months in KOH, almost no change in physical appearance is observed while those aged in DI H_2O starts changing their appearance with dark deposition on the surface as seen in the figure 3.

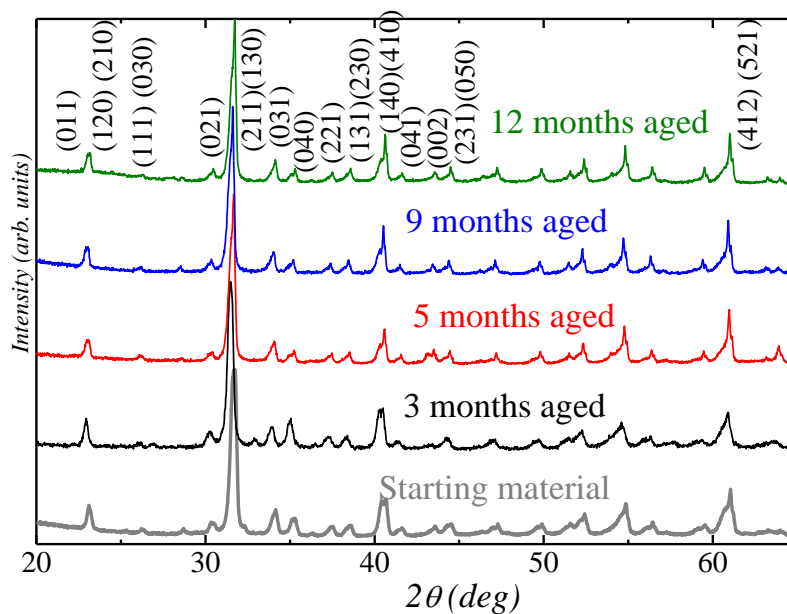


Figure 4: X-Ray diffraction patterns along the KOH ageing period up to 1 year. No noticeable peaks of Gd_2O_3 (JCPDS 12-0797) or other oxides are underline after 12 months ageing.

During its ageing procedure in KOH solution, the $Gd_6Co_{1.67}Si_3$ material has been periodically characterized using X-Ray diffraction knowing that the appearance of a Gd_2O_3 ($Ia-3$; $a=b=c= 10.797(1) \text{ \AA}$ and $\alpha=\beta=\gamma=90^\circ$) [JCPDS 12-0797] as secondary phase would be the result of

a corrosion process [14]. As shown in Figure 4 no noticeable change on the XRD patterns carried out on the aged slab is seen even after 12 months of ageing. Consequently, contrary to DI H₂O exposure, KOH exposure does not result in crystalline Gd₂O₃ formation at surface at least within the limit of detection.

Auger (AES) depth profiles were carried out to check for possible chemical changes on the surface of the sample. The starting material exhibits a thickness of 30 nm of a natural oxidized layer and the nominal composition is reached at the depth of 150 nm (Fig. 5a). The 3 months DI water aged sample reveals a fully oxidized surface up at least to 1200 nm in depth [14]. Only the first 800 nm are shown in Fig. 5b for comparison with Fig. 5c. A significant difference is seen on the 3 months KOH aged sample (Fig. 5c, c') with an oxidized thickness of about only 50 nm. The sharp oxidized surface layer is divided into a rich "Si-O" 20 nm top layer followed by an oxidized mixture involving the Gd, Co and Si elements. Then, a rather quick decrease in oxygen is seen that is similar to the starting material (see figure 5a and 5c') and obviously different from the 3 months DI H₂O aged sample.

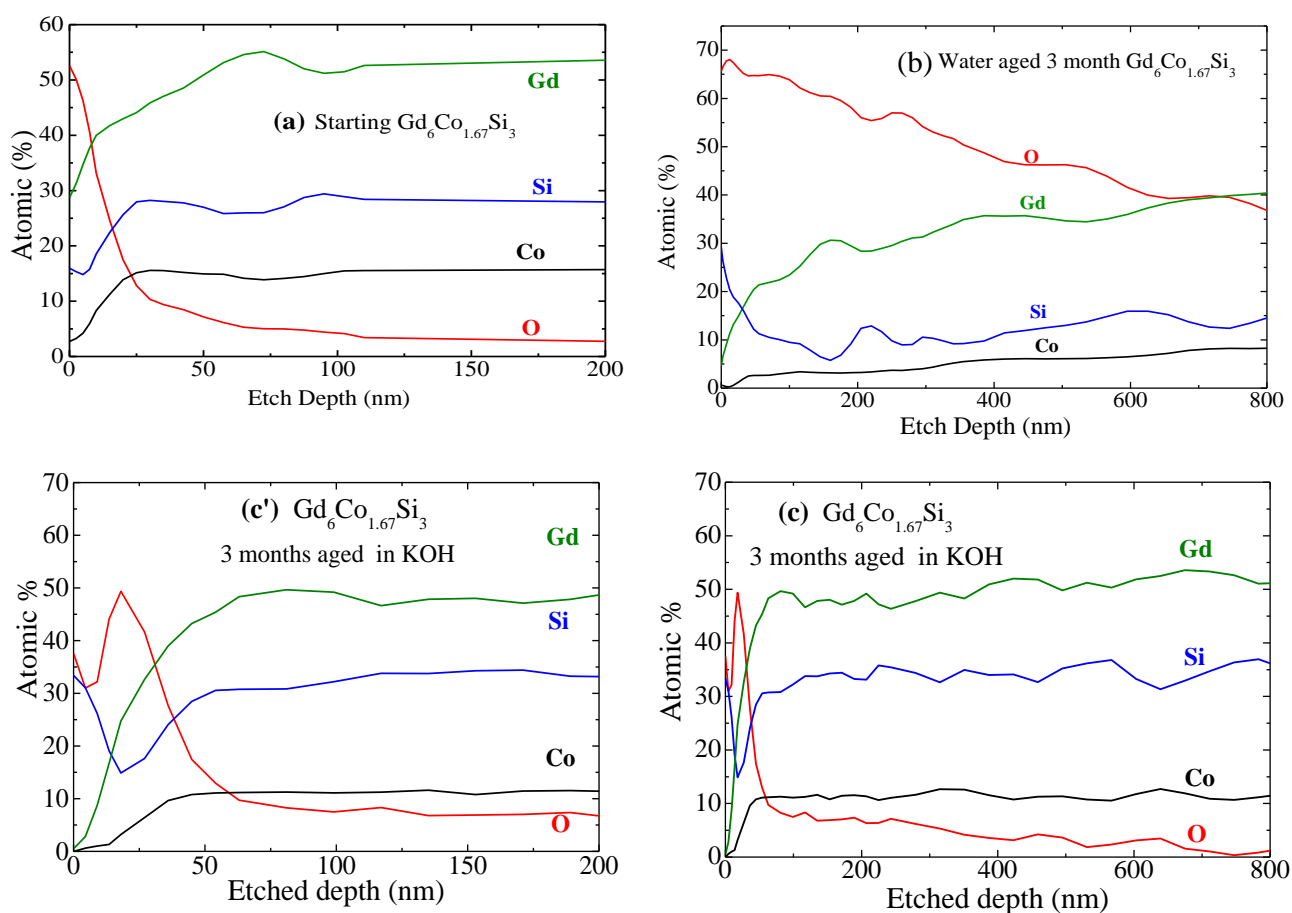


Figure 5: AES depth profiles on (a) starting material, (b) 3 months DI water aged sample, (c)-(c') 3 months KOH aged sample [(c') zoomed area of (c)].

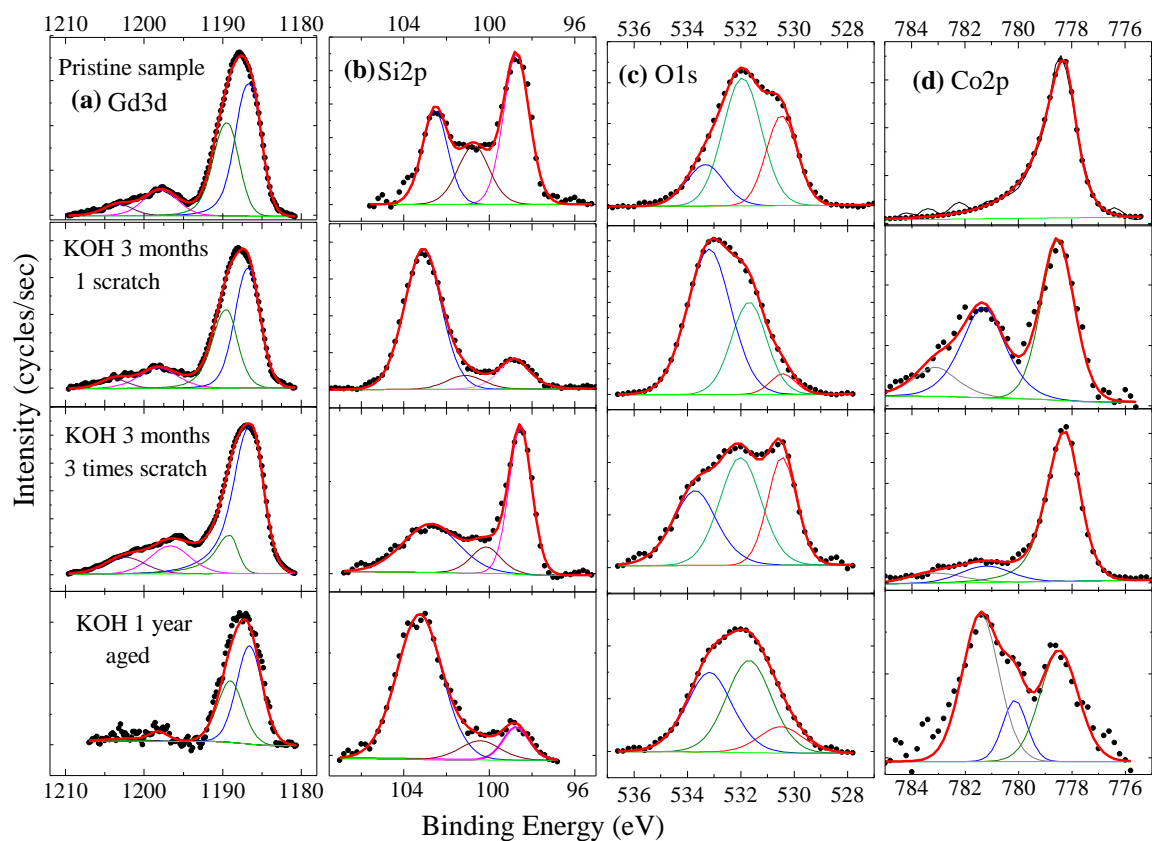


Figure 6: Fitted XPS high-resolution spectra on top surfaces or scratched surfaces for pristine or KOH aged samples. Gd $3d_{5/2}$ column (a), Si $2p$ column (b), O $1s$ column (c) Co $2p_{3/2}$ column (d) from left to right. Experimental data are black symbols lines, fitted envelope or summation is solid red line and individual components are shown in lines with colour variants.

To investigate the chemical environment at the material surface, XPS spectra were collected on pristine, 3 and 12 months KOH aged samples. Data were collected on the top surface and following successive scratch in UHV (Figure 6 a, b, c, d). “Scratch 1” data collected corresponds to measurements carried out after a slight scratch while “Scratch 2” and “Scratch 3” are those after successive further removal of the top surface. XPS spectra following this procedure are summarized in Figure S2 for the 3 months KOH aged sample. Some potassium (K $2p$) trace is only shown after Scratch 1 and disappears with further scratching (Figure S a) which is likely due to some potassium penetration in the sample. Binding energies are discussed taking into account the virgin sample as reference and starting from Gd $3d_{5/2}$ (Fig. 6a) to Co $2p_{3/2}$ (Fig. 6d). Such methodology allows illustrating trends in the corrosion process.

No significant changes in Gd $3d_{5/2}$ XPS spectra through the ageing procedure have been observed. The main peak around 1188 eV is always kept as pointed out by D. Raiser and J.P. Deville [15]. Some Gd $3d_{5/2}$ XPS spectra were collected on Gd metal and Gd $2O_3$ samples as

references (Figure S3 a,b) and the main difference indeed results in a stronger satellite shoulder located around 1195 eV when metallic Gd environment is present. It turns out that this shoulder intensity decrease from the pristine sample to the 1 year KOH aged sample. When scratching the KOH aged samples (Scratch 1 and Scratch 3), XPS $Gd3d_{5/2}$ features move towards the pristine sample one's suggesting gadolinium does not withstand a strong oxidation and thus being protected from corrosion as expected from our XRD analysis.

Silicon environment is followed through $Si2p$ spectra (Figure 6b). The surface oxidation mainly results in SiO_2 formation with an increase of the feature around 103.4 eV. Interestingly, silicon feature around 98.7 eV corresponding to Si^0 in $Gd_6Co_{1.67}Si_3$ is always seen as well as a small one's at intermediate energy. It suggests continuous stabilization of Si^{2+} , Si^+ , Si^0 contributions from top surface to sub-surface indicating that our previous "pristine $Gd_6Co_{1.67}Si_3$ core" / " $Gd_2O_3-SiO_x$ shell" model is found. Top SiO_2 is highlighted with deeper SiO at surface when slabs are exposed to KOH but keeping Si^0 from $Gd_6Co_{1.67}Si_3$ in the probed range scale

$O1s$ fitted spectra reveal 3 different components (Fig. 6c). The one at higher energy around 533 eV is attributed to SiO_2 type bonding in relation with the silicon oxidation ($Si2p$ component at 103.4 eV, Fig. 6b). The one at lower energy around 530.5 eV is associated to a Gd-O type bonding as recorded on natural oxidized Gd metal or on Gd_2O_3 sample (Figure S 3 c, d) while the intermediate one's at 531.7 eV is rather attributed to a Co-O environment close to what is proposed in literature [16]. When the slab is exposed to KOH solution for 3 to 12 months, the relative intensity of the " SiO_2 " $O1s$ feature increases significantly with respect to the two others. It even becomes more prominent after 3 months ageing in KOH as expected from our AES depth profile analysis. When the 3 month in KOH aged sample is scrapped, the " SiO_2 " $O1s$ component decreases in opposition to both Co-O and Gd-O components. Our XPS analysis further supports that $Gd_6Co_{1.67}Si_3$ sample oxidation mainly occurs for silicon when KOH ageing procedure is running.

$Co2p_{3/2}$ spectra are shown Figure 6d. The pristine sample is characteristic of a metallic behavior with one component at 778.3 eV in binding energy. When slabs are exposed to KOH, the $Co2p_{3/2}$ spectrum is complex with likely 3 different components as seen on the "3 months aged after one Scratch" and on the "1 year aged top surface" collected data. With a KOH exposure, a high intense component around 781.3 eV appears, broader than the metallic one's. This is a typical signature of cobalt linked with oxide-hydride or oxygen as quoted in literature

[16]. As both CoO or Co(OH)₂ give Co2p_{3/2} spectra with 780-780.4eV and 782.2eV peaks, and Co₃O₄ gives 3 resolved peaks at 779.6, 780.9 and 782.2 eV, none of these unique compositions are likely found on the top surface. Furthermore, the limit between the Co(OH)₂ and the Co₃O₄ domains is not far from pH = 12 as illustrated in the Pourbaix diagram of cobalt (Fig S1b). Interestingly, the feature around 781.3 eV is almost immediately gone after a moderate scrapped procedure supporting a tiny cobalt oxidized surface. That is why cobalt remains on the top of our slab being mostly in mixed metallic and oxidized forms. Whatever its chemical form, it is highly important to point out that even after 1 year exposure to KOH flux, the cobalt element is still present at surface which was absolutely not the case when slabs were exposed to DI H₂O for 3 months.

Consequently, two important results emerged from our ageing procedure using KOH. The first one is that a slight 25-nm thick SiO₂ component is seen on the top surface from AES depth profiles analysis with a poor gadolinium or cobalt content. Secondly, cobalt element is unambiguously still observed in the sub-surface when the sample is exposed to KOH for one year contrary to what was observed for 3 months in DI H₂O exposure [14]. That is why, our XRD, AES and XPS analysis suggest a corrosion process resulting in a “pristine Gd₆Co_{1.67}Si₃ core” / “(Gd-Co-O_x)-SiO-SiO₂ shell” material with KOH exposure. Our approach to reduce the material corrosion by choosing an appropriate fluid is thus successful. Interestingly, the resulting oxidized top surface thickness is on the same range than the one’s observed when native oxidation of the pristine sample occurs due to air exposure. Let us recall that about 1 μm thick oxide layer does not alter the bulk magnetocaloric effect following a DI H₂O exposure for 3 months. By default, the magnetocaloric effect is thus remained intact following a KOH exposure for one year.

4. Conclusion

The use of dissolved in water potassium hydroxide pellets as heat transport fluid when magnetic refrigeration cycle is mimicked was carried out using Gd₆Co_{1.67}Si₃ material as regenerator. A drastic limitation of the corrosion process is shown. No noticeable crystalline Gd₂O₃ or any other oxides/ hydroxides peaks are seen on the X-Ray diffraction patterns collected on the slab sample that was aged up to 1 year. Further supported by depth profile analyses using AES and detailed XPS spectroscopy, the Gd₆Co_{1.67}Si₃ material is protected by amorphous silica self-coating on the top layer followed in the inner one’s by a mixed

gadolinium/cobalt oxide. These results are consistent with expected spontaneous electrochemical reactions proposed for corrosion effect.

The presented results are of the first of its kind with promising and encouraging contribution towards understanding corrosion and controlling the same by proper choice of heat transport fluid. Our approach dedicated to an ageing test in room temperature magnetic refrigeration (RTMR) $\text{Gd}_6\text{Co}_{1.67}\text{Si}_3$ can be extended to any magnetocaloric intermetallic materials.

Acknowledgment: The authors are grateful to the French ANR-MagCool program for received funding (ANR STKE 2010-008). Madhu Chennabasappa wishes to acknowledge University de Bordeaux 1 for his PhD scholarship.

Supplementary Information

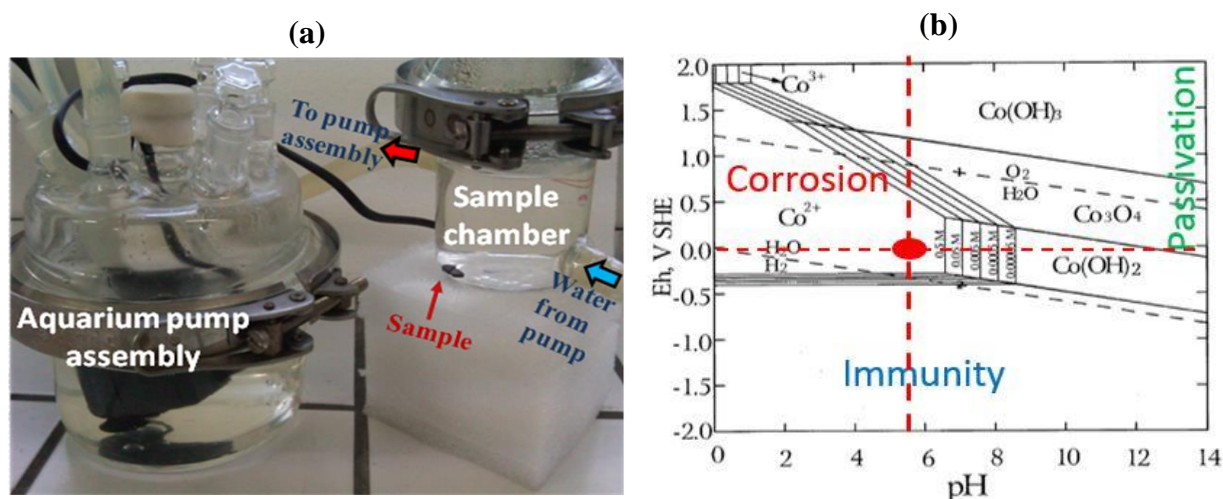


Figure S 1: (a) Photography of the pilot used for water ageing. (b) Pourbaix diagram of cobalt with corrosive, passive and immunity region marking.

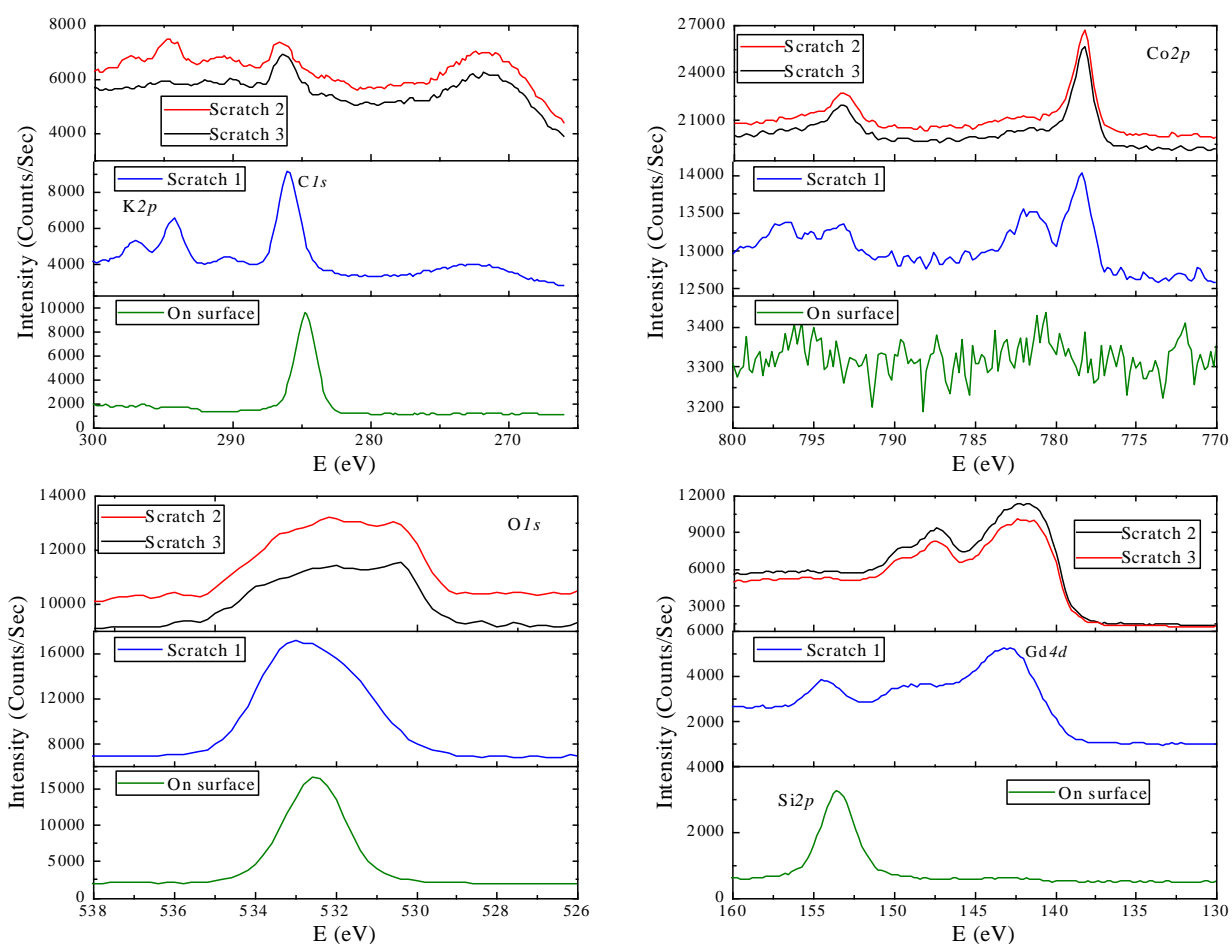
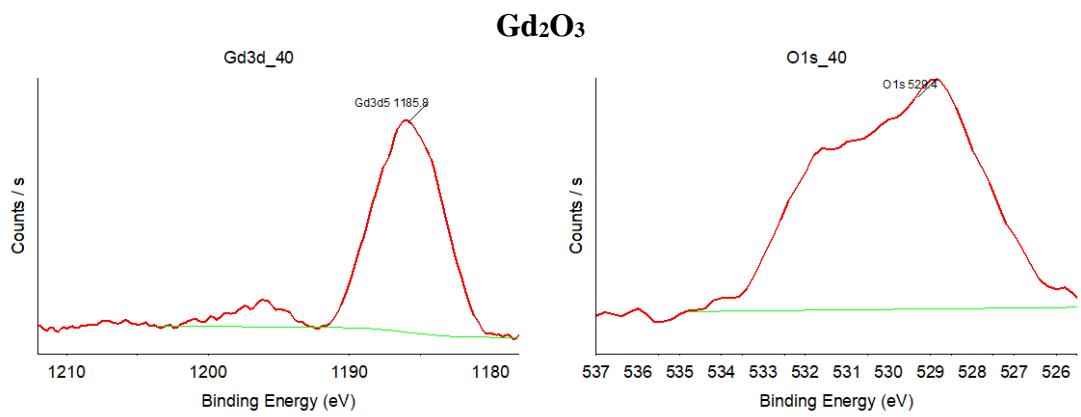
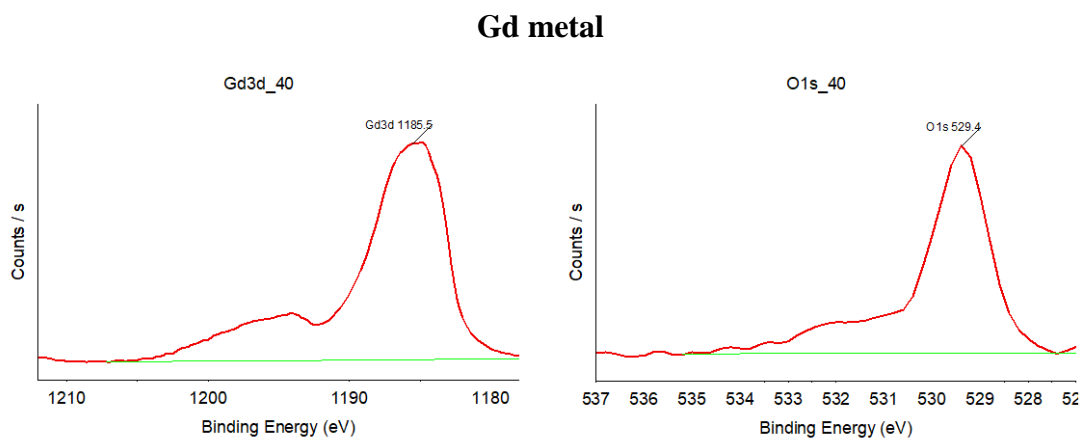


Figure S 2: XPS study on 3 month KOH aged samples to highlight the change in the XPS spectra along depth with respect to the scrapped approach for (a) K2p-C1s-Gd4p3, (b) Co2p, (c) O1s and (d) Si2s-Gd4d.



(a) (c)



(b) (d)

Figure S 3: Comparison of XPS Gd3d_{5/2} spectra (a, b) and O1s spectra (c, d) respectively on Gd₂O₃ and Gd metal.

Schematic demonstrating the corrosion steps	Oxidation/Reduction	E ⁰ (eV)	Electrochemical reaction
	O_2/OH^-	+0.401	$O_2 + 2H_2O + 4e^- \leftrightarrow 4OH^-$ (1)
	Co^{2+}/Co	-0.28	$Co^{2+} + 2e^- \leftrightarrow Co$ (2)
	SiO/Si	-0.80	$SiO + e^- + 2H^+ \leftrightarrow Si + H_2O$ (3)
	$Si^{IV} O_2/SiO$	-0.857	$SiO_2 + 2e^- + 2H^+ \leftrightarrow SiO + H_2O$ (4)
	$Si^{IV} O_3^{2-}/SiO$	-1.697	$SiO_3^{2-} + 4e^- + 4H^+ \leftrightarrow SiO + 2H_2O$ (5)
	Gd^{3+}/Gd	-2.30	$Gd \leftrightarrow Gd^{3+} + 3e^-$ (6)

Table S 1 : Electrochemical reaction details for selected metals and metal oxides along with required potential (E⁰) [16]. [Haynes, W.M., ed. *CRC Handbook of Chemistry and Physics*. 93 ed. 2012 -2013, CRC Press.]

References:

- [1] B.F. Yu, Q. Gao, B. Zhang, X.Z. Meng, Z. Chen, Review on research of room temperature magnetic refrigeration, *International Journal of Refrigeration*, 26 (2003) pp. 622-636.
- [2] A. Smith, Who discovered the magnetocaloric effect?, *Eur. Phys. J. H*, 38 (2013) pp. 507-517.
- [3] R Caballero-Flores, N S Bingham, M H Phan, M A Torija, C Leighton, V Franco, A Conde, T L Phan, S C Yu and H Srikanth *J. Phys.: Condens. Matter* 26 (2014) pp. 286001
- [4] V. Franco, J.S. Blázquez, J.J. Ipus, J.Y. Law, L.M. Moreno-Ramírez, A. Conde Magnetocaloric effect: from materials research to refrigeration devices *Prog. Mater. Sci.*, 93 (2018), pp. 112-232
- [5] A.M. Tishin, Y.I. Spichkin, V.I. Zverev, P.W. Egolf, A review and new perspectives for the magnetocaloric effect: New materials and local heating and cooling inside the human body, *International Journal of Refrigeration*, 68 (2016) pp. 177-186.
- [6] B. Yu, M. Liu, P.W. Egolf, A. Kitanovski, A review of magnetic refrigerator and heat pump prototypes built before the year 2010, *International Journal of Refrigeration*, 33 (2010) pp. 1029-1060.
- [7] A. Kitanovski, J. Tušek, U. Tomc, U. Plaznik, M. Ožbolt, A. Poredoš, Overview of Existing Magnetocaloric Prototype Devices, in: *Magnetocaloric Energy Conversion: From Theory to Applications*, Springer International Publishing, Cham, 2015, pp. 269-330.
- [8] S. Ahmin, M. Alamanza, A. Pasko, F. Mazaleyrat & M. LoBue Thermal energy harvesting system based on magnetocaloric materials *Eur. Phys. J. Appl. Phys.* 85 (2019) pp. 10902

- [9] F. Canepa, S. Cirafici, M. Napoletano, M.R. Cimberle, L. Tagliafico, F. Scarpa, Ageing effect on the magnetocaloric properties of Gd, $Gd_5Si_{1.9}Ge_{2.1}$ and on the eutectic composition $Gd_{75}Cd_{25}$, *Journal of Physics D: Applied Physics*, 41 (2008) pp. 155004.
- [10] M. Zhang, Y. Long, R.-c. Ye, Y.-q. Chang, Corrosion behavior of magnetic refrigeration material La–Fe–Co–Si in distilled water, *Journal of Alloys and Compounds*, 509 (2011) pp. 3627-3631.
- [11] M. Balli, S. Jandl, P. Fournier, and A. Kedous-Lebouc, Advanced materials for magnetic cooling: Fundamentals and practical aspects *Appl. Phys. Rev.* 4, (2017) pp. 021305
- [12] N. Tian, N. N. Zhang, C. Y. You B. Gao, and J. He Magnetic hysteresis loss and corrosion behavior of $LaFe_{11.5}Si_{1.5}$ particles coated with Cu *Journal of Applied Physics* 113, (2013) pp. 103909 ; See also B. Monfared Design and optimization of regenerators of a rotary magnetic refrigeration device using a detailed simulation model *International Journal of Refrigeration* 88 (2018) 260–274
- [13] E. Gaudin, S. Tencé, F. Weill, J. Rodriguez Fernandez, B. Chevalier, Structural and Magnetocaloric Properties of the New Ternary Silicides $Gd_6M_{5/3}Si_3$ with $M = Co$ and Ni , *Chemistry of Materials*, 20 (2008) pp. 2972-2979.
- [14] M. Chennabasappa, B. Chevalier, M. Lahaye, C. Labrugere, O. Toulemonde, A core–shell phenomenon maintain the magnetocaloric properties of the ternary silicide $Gd_6Co_{1.67}Si_3$ during water flux ageing, *Journal of Alloys and Compounds*, 584 (2014) pp. 34-40.
- [15] D. Raiser and J.P. Deville, Study of XPS photoemission of some gadolinium compounds, *Journal of Electron Spectroscopy and Related Phenomena*, 57 (1991) pp. 91-97
- [16] Biesinger Mark C, Payne Brad P, Grosvenor Andrew P, L.W.M. Lau, A.R. Gerson, R.S.C. Smart, Resolving surface chemical states in XPS analysis of first row transition metals, oxides and hydroxides: Cr, Mn, Fe, Co and Ni, *Applied Surface Science*, 257 (2011) pp. 2717-2730.